Published in final edited form as:

Cytoskeleton (Hoboken). 2016 December ; 73(12): 703–711. doi:10.1002/cm.21340.

Microtubule Binding Protein PACRG Plays a Role in Regulating Specific Ciliary Dyneins During Microtubule Sliding

Katsutoshi Mizuno[1], **Erin E. Dymek**[2], and **Elizabeth F. Smith**[2,*]

[1]Center for Developmental Biology, RIKEN 2-2-3 Minatojima-minamimachi, Chuou-ku, Kobe, Japan

[2]Department of Biological Sciences, Class of 1978 Life Sciences Center Dartmouth College, Hanover, New Hampshire

Abstract

The complex waveforms characteristic of motile eukaryotic cilia and flagella are produced by the temporally and spatially regulated action of multiple dynein subforms generating sliding between subsets of axonemal microtubules. Multiple protein complexes have been identified that are associated with the doublet microtubules and that mediate regulatory signals between key axonemal structures, such as the radial spokes and central apparatus, and the dynein arm motors; these complexes include the N-DRC, MIA, and CSC complexes. Previous studies have shown that PACRG (parkin co-regulated gene) forms a complex that is anchored to the axonemal doublet microtubules. Loss of PACRG causes defects in ciliary motility and cilia related diseases. Here, we use an in vitro microtubule sliding assay to demonstrate that PACRG and its interactors are part of a signaling pathway that includes the central apparatus, radial spokes and specific inner dynein arm subforms to control dynein-driven microtubule sliding. Using a biochemical approach, our studies also indicate that PACRG interacts with the radial spokes.

Keywords

PACRG; dynein; cilia; flagella

Introduction

To produce the complex waveforms typical of beating cilia and flagella, the activity of numerous subforms of axonemal dyneins must be regulated along the length and circumference of the axoneme. Substantial evidence indicates that the radial spokes (RSs) and central apparatus (CA) form a signal transduction network that contributes to the regulation of microtubule sliding [reviewed in (Smith and Yang, 2004)].

*Address correspondence to: Elizabeth F. Smith, Department of Biological Sciences, Class of 1978 Life Sciences Center Dartmouth College, Hanover, New Hampshire. elizabeth.f.smith@dartmouth.edu.
Katsutoshi Mizuno's present address is RIKEN 2-2-3 Minatojima-Minamimachi.

All authors have no conflict of interest to declare.

We and others have demonstrated that the repeating pairs of RSs are not homogenous in composition or structure (Dymek *et al.*, 2011; Pigino *et al.*, 2011; Barber *et al.*, 2012; Heuser *et al.*, 2012). We previously identified an adaptor complex specific for radial spoke 2 (RS2) which we named the CSC and which is required for RS2 assembly and stability (Dymek and Smith, 2007; Dymek *et al.*, 2011). Using an in vitro axonemal microtubule sliding assay, we demonstrated that the CSC also plays a role in controlling dynein-driven microtubule sliding and ciliary motility (Dymek and Smith, 2007; Dymek *et al.*, 2011). Other investigators have now provided evidence that the organization and function of the CSC is highly conserved (Urbanska *et al.*, 2015; Vasudevan *et al.*, 2015).

One prediction from these studies is that an analogous regulatory complex is anchored to RS1. Although a specific RS1 adaptor has not been reported, several protein complexes have been characterized which are anchored to the doublet microtubules and likely participate in the conversion of microtubule sliding into ciliary bends. These complexes include the nexin-dynein regulatory complex (N-DRC) as well as the MIA complex. The N-DRC makes physical contact with RSs and outer and inner dynein arms (Heuser *et al.*, 2009). Mutations in some members of this complex suppress paralysis in spokeless and central pairless axonemes indicating a role for this complex in regulating ciliary motility via a signaling pathway that includes these axonemal structures (Piperno *et al.*, 1994). The MIA complex is associated with inner dynein arm I1 and is required for proper I1 assembly (King and Dutcher, 1997; Yamamoto *et al.*, 2013). The MIA complex also makes contact with the N-DRC, suggesting a role for the MIA complex in coordinating cues between the N-DRC and I1 dynein (Yamamoto *et al.*, 2013).

Additional studies have suggested that Rib72, PACRG (the Parkin co-regulated gene product), FAP252, and FAP20 form a complex which is anchored to the doublet microtubules (Ikeda *et al.*, 2007; Yanagisawa *et al.*, 2014). Rib72 was simultaneously discovered by three different labs. The King lab (Patel-King *et al.*, 2002) independently identified Rib72 [p72 in (Patel-King *et al.*, 2002)] as a regulatory subunit of nucleoside-diphosphate kinase. Rib72 has a very conserved structure among eukaryotes; its human homolog is named Efhc1 (Patel-King *et al.*, 2002; Ikeda *et al.*, 2003; Ikeda *et al.*, 2007). Mutations in the EFHC1 ares the cause of juvenile myoclonic epilepsy (Suzuki *et al.*, 2009).

Using biochemical approaches, the Linck lab discovered that Rib72 was a component of “ribbons” of three protofilaments from the A-tubule. The Kamiya lab discovered Rib72 in studies designed to identify the target of proteases used in the sliding assay. These two labs combined their data in a single publication (Ikeda *et al.*, 2003) and demonstrated that not only was Rib72 a component of the protofilament ribbons but that Rib72 epitopes are also exposed on the surface of A-tubule. Remarkably, immunogold labeling showed that these Rib72 epitopes repeat every ~100 nm, the same repeat period as the RSs. More recent localization studies from the Linck and Nicastro labs confirm that Rib72 is associated with a ribbon inside the A-tubule of the microtubule doublet near protofilaments A11-12-13-1 (Linck *et al.*, 2014).

PACRG was originally identified in the human genome as a gene, whose transcription is coregulated with a Parkinson’s disease-related gene Parkin by a bi-directional promoter

(Kitada et al., 1998; West et al., 2003). PACRG has been localized to the axoneme (Dawe *et al.*, 2005; Lechtreck *et al.*, 2009; Thumberger *et al.*, 2012). Loss of PACRG results in male sterility in mice (Lorenzetti *et al.*, 2004) as well as defects in ependymal ciliary motility and hydrocephalus (Wilson *et al.*, 2009; Wilson *et al.*, 2010). RNAi-mediated knockdown of the PACRG gene in *Trypanosoma brucei* results in impaired flagellar motility and defects in doublet microtubule integrity (Dawe *et al.*, 2005). Kamiya's group has provided evidence that PACRG and FAP252 interact with Rib72 (Ikeda *et al.*, 2007). In addition Ikeda has shown that PACRG binds directly to tubulin and microtubules (Ikeda, 2008). More recently, Yanagisawa *et al* have shown that FAP20 is an inner junction protein of the doublets, and that PACRG, but not Rib72, is reduced in FAP20 mutants (Yanagisawa *et al.*, 2014) indicating that FAP20 may also interact with PACRG. FAP20 mutants, like PACRG mutants, have cilia with abnormal motility.

Taken together, these data indicate that Rib72, PACRG, FAP252, and FAP20 form a complex that is associated with the axonemal doublet microtubules and that plays a role in regulating ciliary motility. To test whether this complex (like the CSC, MIA complex, and DRC) mediates regulatory cues from the CA and RSs to the dynein arms, we took advantage of *Chlamydomonas* mutants and an in vitro microtubule sliding assay. Our results reveal that PACRG is a component of the signal transduction pathway that includes the CA, RSs, and specific inner dynein arms.

Results and Discussion

Previous studies have suggested that PACRG interacts with the axonemal protein FAP20, localized at the inner junction of doublet microtubules (Yanagisawa *et al.*, 2014). This location is near the root of the RSs on the A2 and A3 protofilaments (Nicastro *et al.*, 2006; Barber *et al.*, 2012); therefore, it is possible that PACRG and its interactors are involved in relaying signals from the CA and RSs to the inner dynein arms. To test this hypothesis, we used an in vitro microtubule sliding assay with disintegrating axonemes to study the function of PACRG in the regulation of dynein-driven microtubule sliding. Axonemes isolated from the CA defective mutant *pf18* have significantly decreased sliding velocities compared with wild type (Smith, 2002a,b). We have shown previously that antibodies generated against axonemal components can be used in the sliding assay to reveal protein function. For example, addition of antibody against CaM-IP2, a component of the CSC, to *pf18* axonemes restores sliding velocities to wild-type levels (Dymek and Smith, 2007). Therefore, we conducted similar experiments using antibodies generated against PACRG.

We incubated the axonemes isolated from *pf18* with protein A-purified anti-PACRG IgG and performed the sliding assay. In the presence of 15 μg mL^{-1} anti-PACRG antibodies, axonemes of *pf18* showed significantly higher sliding velocities (14.5 ± 0.6 μm s^{-1}, mean ± SEM), compared with the 0 μg mL^{-1} control (10.2 ± 0.3 μm s^{-1}; $P < 0.0001$; Fig. 1A, Table I). In addition, the increase in sliding velocities with anti-PACRG antibody was dose-dependent, indicating that the effect of recovered sliding velocity is specific (Fig. 1B). These results suggest that PACRG is part of signal transduction pathway that includes the CA and dynein arms. Evidently, the requirement for the CA to sustain faster sliding velocities is by-passed by the addition of anti-PACRG antibodies.

Axonemes isolated from the *pf14* mutant which lack RSs also have slow microtubule sliding velocities compared to WT (Smith and Sale, 1992). Our previous studies demonstrated that the addition of anti-CaM-IP2 antibodies to spokeless axonemes isolated from the *pf14* mutant restored WT sliding velocities (Dymek and Smith, 2007). Therefore, we tested whether anti-PACRG antibodies had any effect on *pf14* sliding velocity. Sliding velocities of *pf14* axonemes were significantly increased in the presence of 15 μg mL^{-1} of anti-PACRG antibodies (12.6 ± 0.6 μm s^{-1}) compared with the 0 μg mL^{-1} control (10.0 ± 0.4 μm s^{-1}; $P < 0.0001$; Fig. 1A). Like *pf18* axonemes the increase in sliding velocities of *pf14* axonemes with anti-PACRG antibody was dose-dependent, indicating that the effect of recovered sliding velocity is specific (Fig. 1C). Western blots using the anti-PACRG, ant-Rib72, and anti-FAP252 antibodies and isolated axonemes reveal that the antibodies are highly specific (Fig. 1D). These combined results strongly indicate that PACRG is part of a signal transduction pathway that includes the RSs as well as the CA and dynein arms.

On the basis of the report that PACRG may form a complex with Rib72 and FAP252, we used antibodies generated against these proteins in the same axoneme sliding disintegration assay. We discovered that both anti-Rib72 and anti-FAP252 antibodies significantly increase sliding velocity of *pf18* axonemes with anti-Rib72 antibodies increasing velocities to nearly WT levels (Fig. 1A). In addition, anti-Rib72 but not anti-FAP252, antibodies significantly increase sliding velocity to *pf14* axonemes (Fig. 1A). These results provide additional evidence that PACRG and associated proteins are components of a complex that regulate microtubule sliding.

To determine if PACRG mediates regulatory cues to specific subsets of dynein arms, we repeated the sliding experiment using axonemes isolated from the double mutant *pf18pf28* (Table I). These axonemes lack the CA and outer dynein arms. Sliding velocities for *pf18pf28* axonemes are significantly slower than *pf18* axonemes. However, velocities did not increase in response to addition of ant-PACRG antibodies. This result may indicate that the outer dynein arms are possible targets for regulation by PACRG. However, it should be noted that velocities are low and many axonemes do not undergo sliding. Therefore, the axoneme number for these experiments is low compared to other strains.

To determine if PACRG mediates regulatory cues to specific subsets of inner dynein arm subforms we performed the microtubule sliding assay using double mutants that lack the CA or RSs and specific dynein subforms (Fig. 2, Table I). The inner dynein arm mutants include *ida1* or *pf30* which both lack dynein I1/f (Piperno *et al.*, 1990; Kamiya *et al.*, 1991; Kagami and Kamiya, 1992; Porter *et al.*, 1992), *ida4* which lacks dynein subforms a, c, and d (Kamiya *et al.*, 1991; Kagami and Kamiya, 1992; Piperno *et al.*, 1992; Porter *et al.*, 1992), *ida9* which lacks dynein subform c (Yagi *et al.*, 2005), and *ida6* which lacks dynein arm subform e (Kato *et al.*, 1993; Yanagisawa and Kamiya, 2004). Addition of anti-PACRG antibody to axonemes from double mutants lacking both the CA and dynein I1/f (*pf18ida1*) increased sliding velocity to a similar extent in *pf18* single mutants (Fig. 2A). Addition of anti-PACRG antibody to double mutants lacking the RSs and dynein I1/ f (*pf14pf30*) also increased sliding velocities (Fig. 2B). These results suggest that dynein I1/f is not the target of regulation by PACRG. These results are in contrast to our results with anti CaM-IP2

antibodies; anti-Cam-IP2 antibodies failed to increase sliding velocities in *pf18ida1* and *pf14pf30* mutants (Dymek and Smith, 2007).

Addition of anti-PACRG antibodies to axonemes isolated from *pf18ida4* mutant that lack the CA and dynein subforms a, c, and d, failed to increase sliding velocity (Fig. 2A). This result indicates that inner dynein arms a, c, and/ or d are candidate targets for regulation by PACRG. Note that this result is in contrast to those we obtained for anti-CaM-IP2 antibodies; CaM-IP2 antibodies increase sliding velocities in *pf18ida4* axonemes (Dymek and Smith, 2007). We also generated a double mutant lacking the CA (*pf18*) and dynein subform c (*ida9*). Addition of anti-PACRG antibodies to axonemes isolated from this strain did increase sliding velocities. Therefore, inner arm dynein subforms a and/or d must be the targets of this regulation. No mutants are currently available which would allow us to distinguish between inner dynein arm subforms a and d. Interestingly, dyneins a and d are near RS1.

We also performed the same experiments using axonemes isolated from *pf18ida1* and *pf18ida4* with both the anti-FAP252 and anti-RIB72 antibodies. In all cases we obtained the same results that we obtained with the anti-PACRG antibodies. Both antibodies increase sliding velocity for *pf18ida1* but not for *pf18ida4* (Fig. 2A). Taken together these results indicate that the PACRG complex, like the CSC, mediates regulatory signals that include the CA, RSs, and dynein arms. However, an important difference is that these two complexes impact upon different dynein subforms.

We also tested axonemes isolated from the double mutant *pf18ida6*, which lack both the CA and dynein e. To our surprise in the control experiment without antibody addition, *pf18ida6* axonemes had significantly faster sliding velocities than the *pf18* axonemes ($P < 0.0001$ Fig. 2A). Evidently the loss of inner dynein arm subform e alone can suppress the slow sliding velocities that result from the loss of the CA. It should be noted that the *ida6* mutation is in the gene encoding FAP250 which is likely the DRC2 subunit of the dynein regulatory complex subunit (Austin-Tse *et al.*, 2013). This defect may also account for the apparent suppression of *pf18* slow sliding velocity in the *pf18ida6* mutant.

These results combined with those of previous investigators indicate that PACRG and its interactors are localized to the doublet microtubules in a position to mediate regulatory cues between the radial spokes and dynein arms. On the basis of the possible regulation of inner dynein arms a and/or d and based on our work with CSC components, we hypothesized that the PARCG complex may be associated with the RSs and potentially with RS1. This hypothesis is supported by the observation that immunogold labeling showed that Rib72 epitopes repeat every ~100nm, the same repeat period as the RSs (Ikeda *et al.*, 2003). To determine if PACRG interacts directly with RSP3, a radial spoke protein located at the base of the spokes and which interacts directly with the CSC at the base of RS2, we performed a gel overlay assay using bacterially expressed proteins. In this assay PACRG binds to RSP3 (Fig. 3).

To obtain additional evidence of interaction between the PACRG complex and the radial spokes, we also performed immunoprecipitations experiments using antibodies generated

against PACRG, FAP252, and Rib72. We were unable to consistently precipitate RS proteins using these antibodies (not shown). We also examined the sedimentation profile of PACRG, FAP252, and Rib72 in axonemal extracts subjected to sucrose density gradient centrifugation (Fig. 4). PACRG is present in a number of fractions including those at 21S which contain RS proteins. Of note, when extracts are prepared from the radial spokeless mutant *pf14*, no PACRG is present at 21S, further suggesting an interaction with the spokes. In extracts prepared form WT axonemes, FAP252 and Rib72 sediment closer to 10S. If these proteins form a complex with PACRG and the RSs, the complex is unstable under our conditions of extraction and density gradient centrifugation.

Our combined results provide evidence that PACRG forms an axoneme associated complex that mediates signals from the radial spokes and central apparatus to regulate dynein-drive microtubule sliding. On the basis of the fact that PACRG interacts with RSP3 in vitro and given the specific inner dynein arms that are required for this regulation, we predict that PACRG and potential complex members are associated with or close to RS1. Testing this prediction will require generating new reagents and strains.

Materials and Methods

Chlamydomonas Reinhardtii Strains

Chlamydomonas strain A54-e18 (*nit1-1, ac17, sr1*, mt+) was used as wild-type and obtained from Paul A. Lefebvre (University of Minnesota, St. Paul, MN). The central pair-defective strain *pf18*, the radial spoke-defective stain *pf14*, and the dynein-defective strains *ida1, ida4, ida6*, and *ida9* were obtained from the *Chlamydomonas* Genetics Center (University of Minnesota, Minneapolis, MN). The *pf14pf30* strain was obtained from Winfield S. Sale (Emory University, Atlanta, GA). Generation of the double mutants *pf18ida1* and *pf18pf28* have been previously described (Smith, 2002b). The *pf18ida4, pf18ida6*, and *pf18ida9* strains were selected from tetrads as non-motile cells and then screened by western blotting. All cells are grown in constant light in Tris acetate phosphate (TAP) media (Gorman and Levine, 1965).

Preparation of Flagella, Flagellar Extracts, and Sucrose Gradients

Flagella were severed from cell bodies by the dibucaine method (Witman, 1986) and isolated by differential centrifugation in NaLow buffer (10 mM Hepes, pH 7.4, 5 mM $MgSO_4$, 1 mM dithiothreitol [DTT], 0.5 mM EDTA, and 30 mM NaCl). Axonemes were obtained by demembanating flagella by adding NP-40 (Calbiochem, La Jolla, CA) for a final concentration of 0.5%. KI extracts (after 2 NaCl extractions) were obtained as previously described (Dymek and Smith, 2007). For sucrose gradient centrifugation, KI extracts were loaded onto a 5–20% sucrose gradient in NaLow and centrifuged at 35,000 rpm for 16 hr in a SW41Ti rotor (Beckman Coulter, Brea, CA). The 0.6 mL fractions were collected from the bottom of the tube and prepared for SDS-PAGE.

Gel Electrophoresis and Western Blotting

Samples were resolved on polyacrylamide gels and transferred to polyvinylidene difluoride membrane (Immobilon-P; Millipore, Billertica, MA). For western blotting, membranes were

blocked in 5% milk/TBST (0.1% Tween/Tris-buffered saline, pH 7.5). Primary antibodies were diluted into TBST. The following dilutions were used: anti-PACRG, 1:40,000; anti-FAP252, 1:10,000 (anti-PACRG and anti-FAP252 antibodies were generously provided by Masafumi Hirono, Hosei University, Tokyo, Japan); anti-Rib72, 1:10,000 (generously provided by Stephen M. King, Univ. of Connecticut Health Center); affinity purified anti-CaM-IP3, 1:1000 (Dymek and Smith, 2007); anti-RSP5, 1:5,000 (generously provided by Dennis R. Diener, Yale University). For western blots of axonemes, purified anti-PACRG, -Rib72, or -FAP252 were used at 1:5000. Anti-rabbit-HRP (GE Healthcare, Piscataway, NJ) was used as the secondary antibody at 1:30,000 in TBST. ECL Prime Western Blotting Detection reagent (GE Healthcare) was used for detection according to the manufacturer's instructions.

Gel Overlay Assay

RSP3-GST (generously provided by Win Sale, Emory University) and the amino terminus of His-CaM-IP2 were expressed and purified as described in Dymek and Smith (2007). His-FAP221 (two tandem repeats of the C-terminus) was expressed and purified according to DiPetrillo and Smith (DiPetrillo and Smith, 2010). Full length PACRG was acquired using RT-PCR. The amplified PCR product was subcloned into pCR2.1 and sequenced. The PACRG clone was shuttled to pET30a, sequenced and transformed into BL21 (DE3) pLysS cells for expression. Expression was induced with 1 mM IPTG and protein was purified from bacterial cell lysates using a Ni^{2+}-resin column (Novagen, Madison, WI). For SDS-PAGE, 30 μg of FAP221, 10 μg of CaM-IP2, and 10 μg of His-PACRG were resolved on an 11% polyacrylamide gel and transferred to nitrocellulose membrane. Membranes were blocked overnight at 4°C in 5% milk/TBST (0.1% Tween) then incubated with RSP3-GST (40 μg mL^{-1}) in 1% BSA/TBST for 2 hours at RT. After 3 × 5 min TBSTwashes, membranes were incubated with anti-GST-HRP (1:7500) in TBST for 1 h. Blots were washed 3 × 5 min TBST then the ECL Plus Western Blotting kit was used for detection (GE Healthcare, Piscataway, NJ).

Microtubule Sliding Assay

Flagella were isolated from cell bodies by the dibucaine method (Witman, 1986) in KLow buffer (10 mM HEPES, pH 7.4, 5 mM $MgSO_4$, 1 mM DTT, 0.5 mM EDTA, and 25 mM potassium acetate). Axonemes were isolated by adding NP-40 (Calbiochem, La Jolla, CA) to flagella for final concentration of 0.5% just before the sliding experiment. Microtubule sliding was initiated with KLow buffer containing 1 mM ATP and 4 μg mL^{-1} type VIII protease (Sigma-Aldrich, St. Louis, MO). For experiments with antibodies, axonemes were incubated with protein A-purified anti-PACRG antibodies (15 μg mL^{-1} or various doses), anti-FAP252 antibodies (15 μg mL^{-1}), or affinity purified anti-Rib72 antibodies (15 μg mL^{-1}) for 15 min at room temperature (22°C) before the induction of sliding. For control experiments, the same volume of phosphate buffered saline (PBS) was added. Measurement of sliding velocity between doublet microtubules was based on the methods of Okagaki and Kamiya (1986). Sliding was observed and recorded using an AxioSkop 2 microscope (Carl Zeiss, Thornwood, NY) equipped for darkfield optics including a Plan-Apochromat 40× oil immersion objective with iris and ultra-dark field oil immersion condenser. A silicon-intensified target camera (VE-1000 SIT, Dage-MTI) or an ORCA-Flash 4.0 V2

(Hamamatsu) camera were used for capturing images. Distance of sliding was measured using ImageJ software, and velocity was calculated as a function of change in time. All data are presented as mean ± SEM. All sliding experiments represent the result of three to six independent experiments with a total number for each strains and condition of between 50 and 265. The Tukey's HSD test method was used to determine the significance of differences between means in multiple comparisons. The *t* test was used for the comparison of two independent groups.

Acknowledgments

The authors gratefully acknowledge the technical support of Christine Hodge. This work was supported by the Postdoctoral Fellowships for Research Abroad from the Japan Society for the Promotion of Science (to K.M.) and NIH RO1GM112050 (to E.F.S.).

References

Austin-Tse C, Halbritter J, Zariwala MA, Gilberti RM, Gee HY, Hellman N, Pathak N, Liu Y, Panizzi JR, Patel-King RS, Tritschler D, Bower R, O'Toole E, Porath JD, Hurd TW, Chaki M, Diaz KA, Kohl S, Lovric S, Hwang DY, Braun DA, Schueler M, Airik R, Otto EA, Leigh MW, Noone PG, Carson JL, Davis SD, Pittman JE, Ferkol TW, Atkinson JJ, Olivier KN, Sagel SD, Dell SD, Rosenfeld M, Milla CE, Loges NT, Omran H, Porter ME, King SM, Knowles MR, Drummond IA, Hildebrandt F. Zebrafish ciliopathy screen plus human mutational analysis identifies C21orf59 and CCDC65 defects as causing primary ciliary dyskinesia. Am J Hum Genet. 2013; 93:672–686. [PubMed: 24094744]

Barber CF, Heuser T, Carbajal-Gonzalez BI, Botchkarev VV Jr, Nicastro D. Three-dimensional structure of the radial spokes reveals heterogeneity and interactions with dyneins in *Chlamydomonas flagella*. Mol Biol Cell. 2012; 23:111–120. [PubMed: 22072792]

Bui KH, Yagi T, Yamamoto R, Kamiya R, Ishikawa T. Polarity and asymmetry in the arrangement of dynein and related structures in the *Chlamydomonas axoneme*. J Cell Biol. 2012; 198:913–925. [PubMed: 22945936]

Dawe HR, Farr H, Portman N, Shaw MK, Gull K. The Parkin coregulated gene product, PACRG, is an evolutionarily conserved axonemal protein that functions in outer-doublet microtubule morphogenesis. J Cell Sci. 2005; 118:5421–5430. [PubMed: 16278296]

DiPetrillo CG, Smith EF. Pcdp1 is a central apparatus protein that binds Ca(2+)-calmodulin and regulates ciliary motility. J Cell Biol. 2010; 189:601–612. [PubMed: 20421426]

Dymek EE, Heuser T, Nicastro D, Smith EF. The CSC is required for complete radial spoke assembly and wild-type ciliary motility. Mol Biol Cell. 2011; 22:2520–2531. [PubMed: 21613541]

Dymek EE, Smith EF. A conserved CaM- and radial spoke associated complex mediates regulation of flagellar dynein activity. J Cell Biol. 2007; 179:515–526. [PubMed: 17967944]

Gorman DS, Levine RP. Cytochrome f and plastocyanin: Their sequence in the photosynthetic electron transport chain of *Chlamydomonas reinhardtii*. Proc Natl Acad Sci USA. 1965; 54:1665–1669. [PubMed: 4379719]

Heuser T, Dymek EE, Lin J, Smith EF, Nicastro D. The CSC connects three major axonemal complexes involved in dynein regulation. Mol Biol Cell. 2012; 23:3143–3155. [PubMed: 22740634]

Heuser T, Raytchev M, Krell J, Porter ME, Nicastro D. The dynein regulatory complex is the nexin link and a major regulatory node in cilia and flagella. J Cell Biol. 2009; 187:921–933. [PubMed: 20008568]

Ikeda T. Parkin-*co*-regulated gene (PACRG) product interacts with tubulin and microtubules. FEBS Lett. 2008; 582:1413–1418. [PubMed: 18387367]

Ikeda K, Brown JA, Yagi T, Norrander JM, Hirono M, Eccleston E, Kamiya R, Linck RW. Rib72, a conserved protein associated with the ribbon compartment of flagellar A-microtubules and potentially involved in the linkage between outer doublet microtubules. J Biol Chem. 2003; 278:7725–7734. [PubMed: 12435737]

Ikeda K, Ikeda T, Morikawa K, Kamiya R. Axonemal localization of Chlamydomonas PACRG, a homologue of the human Parkin-coregulated gene product. Cell Motility Cytoskeleton. 2007; 64:814–821.

Kagami O, Kamiya R. Translocation and rotation of microtubules caused by multiple species fo Chlamydomonas inner-arm dynein. J Cell Sci. 1992; 103:653–664.

Kamiya R, Kurimoto E, Muto E. Two types of Chlamydomonas flagellar mutants missing different components of inner-arm dynein. J Cell Biol. 1991; 112:441–447. [PubMed: 1825085]

Kato T, Kagami O, Yagi T, Kamiya R. Isolation of two species of *Chlamydomonas reinhardtii* flagellar mutants, ida5 and ida6, that lack a newly identified heavy chain of the inner dynein arm. Cell Struct Funct. 1993; 18:371–377. [PubMed: 8033218]

King SJ, Dutcher SK. Phosphoregulation of an inner dynein arm complex in *Chlamydomonas reinhardtii* is altered in phototactic mutant strains. J Cell Biol. 1997; 136:177–191. [PubMed: 9008712]

Kitada T, Asakawa S, Hattori N, Matsumine H, Yamamura Y, Minoshima S, Yokochi M, Mizuno Y, Shimizu N. Mutations in the parkin gene cause autosomal recessive juvenile parkinsonism. Nature. 1998; 392(1993):605–608. [PubMed: 9560156]

Lechtreck KF, Luro S, Awata J, Witman GB. HA-tagging of putative flagellar proteins in *Chlamydomonas reinhardtii* identifies a novel protein of intraflagellar transport complex B. Cell Motility Cytoskeleton. 2009; 66:469–482.

Linck R, Fu X, Lin J, Ouch C, Schefter A, Steffen W, Warren P, Nicastro D. Insights into the structure and function of ciliary and flagellar doublet microtubules: Tektins, Ca2+-binding proteins and stable protofilaments. J Biol Chem. 2014; 289:17427–17444. [PubMed: 24794867]

Lorenzetti D, Bishop CE, Justice MJ. Deletion of the Parkin coregulated gene causes male sterility in the quaking(viable) mouse mutant. Proc Natl Acad Sci USA. 2004; 101:8402–8407. [PubMed: 15148410]

Nicastro D, Schwartz C, Pierson J, Gaudette R, Porter ME, McIntosh JR. The molecular architecture of axonemes revealed by cryoelectron tomography. Science. 2006; 313:944–948. [PubMed: 16917055]

Okagaki T, Kamiya R. Microtubule sliding in mutant *Chlamydomonas axonemes* devoid of outer or inner dynein arms. J Cell Biol. 1986; 103:1895–1902. [PubMed: 2946702]

Patel-King RS, Benashski SE, King SM. A Bipartite Ca2+-regulated nucleoside-diphosphate kinase system within the *Chlamydomonas flagellum*. The regulatory subunit p72. J Biol Chem. 2002; 277:34271–34279. [PubMed: 12095989]

Pigino G, Bui KH, Maheshwari A, Lupetti P, Diener D, Ishikawa T. Cryoelectron tomography of radial spokes in cilia and flagella. J Cell Biol. 2011; 195:673–687. [PubMed: 22065640]

Piperno G, Mead K, LeDizet M, Moscatelli A. Mutations in the “dynein regulatory complex” alter the ATP-insensitive binding sites for inner arm dyneins in *Chlamydomonas axonemes*. J Cell Biol. 1994; 125:1109–1117. [PubMed: 8195292]

Piperno G, Mead K, Shestak W. The inner dynein arms I2 interact with a “dynein regulatory complex” in *Chlamydomonas flagella*. J Cell Biol. 1992; 118:1455–1463. [PubMed: 1387875]

Piperno G, Ramanis Z, Smith EF, Sale WS. Three distinct inner dynein arms in *Chlamydomonas flagella*: Molecular composition and location in the axoneme. J Cell Biol. 1990; 110:379–389. [PubMed: 2137128]

Porter ME, Power J, Dutcher SK. Extragenic suppressors of paralyzed flagellar mutations in *Chlamydomonas reinhardtii* identify loci that alter the inner dynein arms. J Cell Biol. 1992; 118:1163–1176. [PubMed: 1387404]

Smith EF. Regulation of flagellar dynein by calcium and a role for an axonemal calmodulin and calmodulin-dependent kinase. Mol Biol Cell. 2002a; 13:3303–3313. [PubMed: 12221134]

Smith EF. Regulation of flagellar dynein by the axonemal central apparatus. Cell Motility Cytoskeleton. 2002b; 52:33–42.

Smith EF, Sale WS. Regulation of dynein-driven microtubule sliding by the radial spokes in flagella. Science. 1992; 257:1557–1559. [PubMed: 1387971]

Smith EF, Yang P. The radial spokes and central apparatus: Mechano-chemical transducers that regulate flagellar motility. Cell Motility Cytoskeleton. 2004; 57:8–17.

Suzuki T, Miyamoto H, Nakahari T, Inoue I, Suemoto T, Jiang B, Hirota Y, Itohara S, Saido TC, Tsumoto T, Sawamoto K, Hensch TK, Delgado-Escueta AV, Yamakawa K. Efhc1 deficiency causes spontaneous myoclonus and increased seizure susceptibility. Hum Mol Genet. 2009; 18:1099–1109. [PubMed: 19147686]

Thumberger T, Hagenlocher C, Tisler M, Beyer T, Tietze N, Schweickert A, Feistel K, Blum M. Ciliary and non-ciliary expression and function of PACRG during vertebrate development. Cilia. 2012; 1:13. [PubMed: 23351225]

Urbanska P, Song K, Joachimiak E, Krzemien-Ojak L, Koprowski P, Hennessey T, Jerka-Dziadosz M, Fabczak H, Gaertig J, Nicastro D, Wloga D. The CSC proteins FAP61 and FAP251 build the basal substructures of radial spoke 3 in cilia. Mol Biol Cell. 2015; 26:1463–1475. [PubMed: 25694453]

Vasudevan KK, Song K, Alford LM, Sale WS, Dymek EE, Smith EF, Hennessey T, Joachimiak E, Urbanska P, Wloga D, Dentler W, Nicastro D, Gaertig J. FAP206 is a microtubule-docking adapter for ciliary radial spoke 2 and dynein c. Mol Biol Cell. 2015; 26:696–710. [PubMed: 25540426]

West AB, Lockhart PJ, O'Farell C, Farrer MJ. Identification of a Novel Gene Linked to Parkin via a Bi-directional Promoter. Journal of Molecular Biology. 2003; 326(1):11–19. [PubMed: 12547187]

Wilson GR, Tan JT, Brody KM, Taylor JM, Delatycki MB, Lockhart PJ. Expression and localization of the Parkin coregulated gene in mouse CNS suggests a role in ependymal cilia function. Neurosci Lett. 2009; 460:97–101. [PubMed: 19463890]

Wilson GR, Wang HX, Egan GF, Robinson PJ, Delatycki MB, O'Bryan MK, Lockhart PJ. Deletion of the Parkin coregulated gene causes defects in ependymal ciliary motility and hydrocephalus in the quakingviable mutant mouse. Hum Mol Genet. 2010; 19:1593–1602. [PubMed: 20106870]

Witman GB. Isolation of Chlamydomonas flagella and flagellar axonemes. Methods Enzymol. 1986; 134:280–290. [PubMed: 3821567]

Yagi T, Minoura I, Fujiwara A, Saito R, Yasunaga T, Hirono M, Kamiya R. An axonemal dynein particularly important for flagellar movement at high viscosity. Implications from a new Chlamydomonas mutant deficient in the dynein heavy chain gene DHC9. J Biol Chem. 2005; 280:41412–41420. [PubMed: 16236707]

Yamamoto R, Song K, Yanagisawa HA, Fox L, Yagi T, Wirschell M, Hirono M, Kamiya R, Nicastro D, Sale WS. The MIA complex is a conserved and novel dynein regulator essential for normal ciliary motility. J Cell Biol. 2013; 201:263–278. [PubMed: 23569216]

Yanagisawa HA, Kamiya R. A tektin homologue is decreased in chlamydomonas mutants lacking an axonemal inner-arm dynein. Mol Biol Cell. 2004; 15:2105–2115. [PubMed: 14978211]

Yanagisawa HA, Mathis G, Oda T, Hirono M, Richey EA, Ishikawa H, Marshall WF, Kikkawa M, Qin H. FAP20 is an inner junction protein of doublet microtubules essential for both the planar asymmetrical waveform and stability of flagella in Chlamydomonas. Mol Biol Cell. 2014; 25:1472–1483. [PubMed: 24574454]

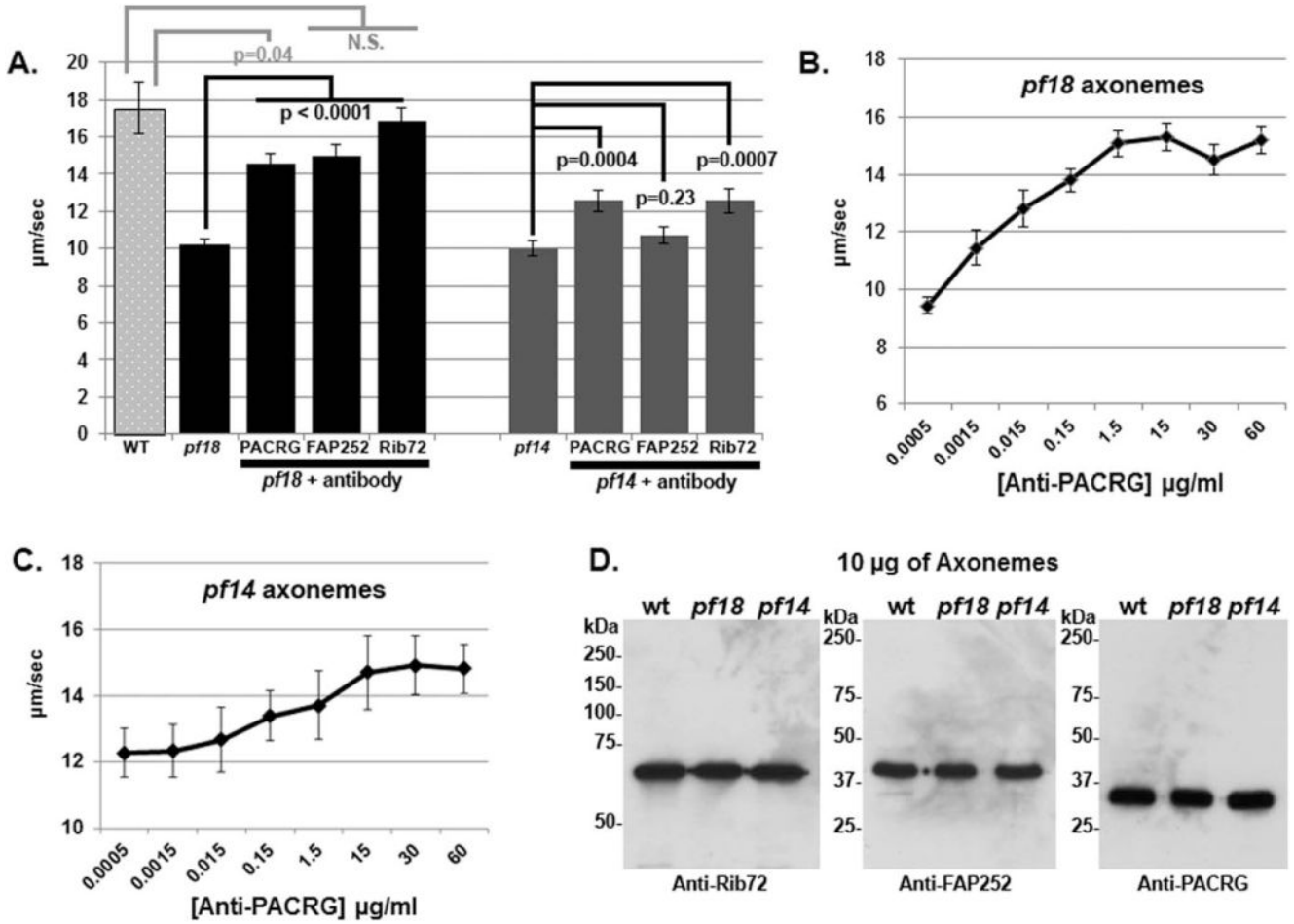

Fig. 1. Antibodies against PACRG, FAP252, and Rib72 increase dynein-driven microtubule sliding velocities of *pf18* and *pf14* axonemes

(**A**) Microtubule sliding velocities of *pf18* and *pf14* axonemes treated with anti-PACRG, -FAP252, and -Rib72. Each antibody significantly increases sliding velocities of *pf18* axonemes. Only anti-PACRG and anti–Rib72 antibodies significantly increase sliding velocities of *pf14* axonemes. N.S. = not significantly different. (**B**/**C**) Anti-PACRG antibodies increase microtubule sliding velocities in *pf18* (B) and *pf14* (C) axonemes in a dose-dependent manner. Microtubule sliding reaches a maximum velocity at ~15 µg mL^{-1} of antibody. Note: since the increase in velocity is smaller for *pf14* axonemes the y-axes of B and C differ in scale. (**D**) Western blots of wt, *pf18*, and *pf14* axonemes using purified anti-Rib72, -FAP252, and -PACRG antibodies. Each antibody recognizes a single protein of the correct size, with minimal background.

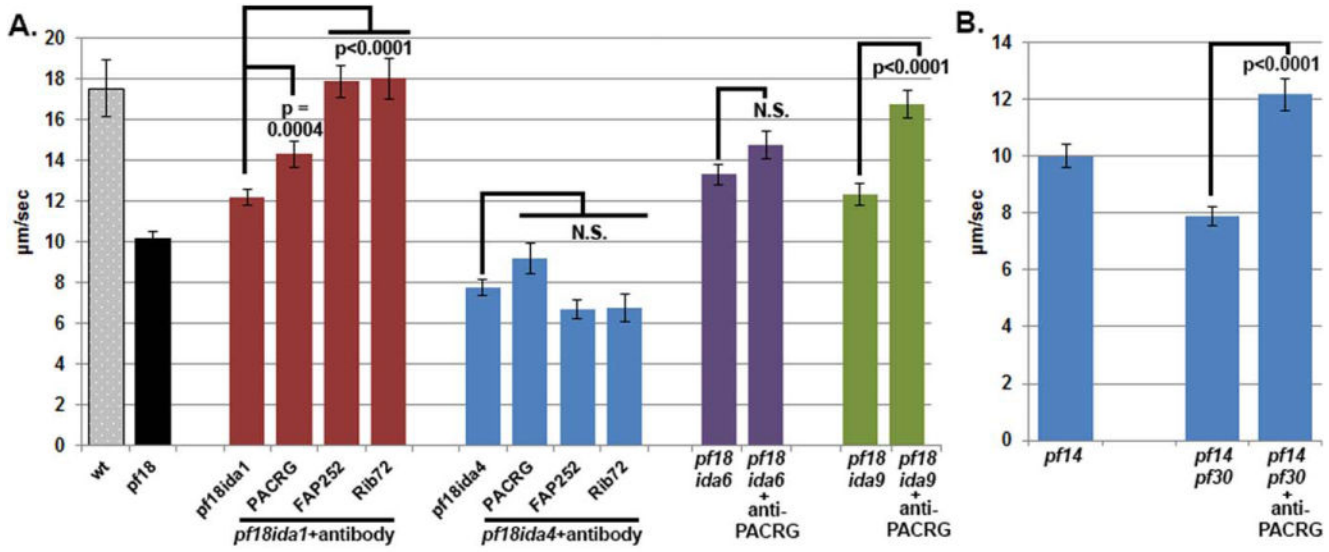

C.

Mutant	Missing Structures	↑Velocity with Anti-PACRG
pf18ida1	central pair, dynein f	Yes
pf18ida4	central pair, dynein a, c, d	No
pf18ida6	central pair, dynein e	No
pf18ida9	central pair, dynein c	Yes
pf14pf30	radial spokes, dynein f	Yes

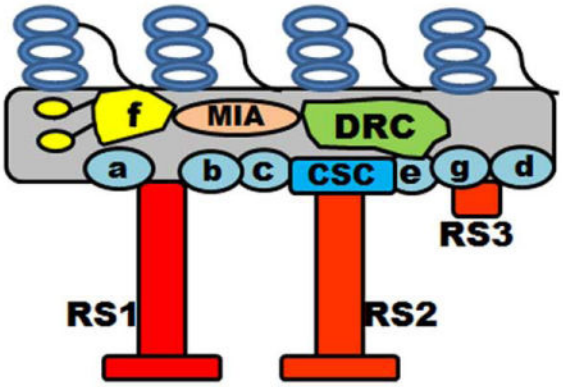

Fig. 2. Microtubule sliding velocities of axonemes with defects in inner dynein arms

(**A**) Microtubule sliding velocities of axonemes lacking the CA and specific inner dynein arms. Dyneins IDA f (*pf18ida1* results) and IDA c (*pf18ida9* results) are not required to increase sliding velocity of *pf18* axonemes treated with antibodies to the PACRG complex. No increase in velocity is observed in *pf18ida4* axonemes (lacking IDA a,c,d) or *pf18ida6* (lacking IDA e). Note that *pf18ida6* axonemes have a faster initial velocity compared to *pf18* mutant axonemes. N.S. = not significantly different (**B**) Microtubule sliding velocities of *pf14* and *pf14ida1* axonemes. Dynein f is not required for an increase in velocity after addition of anti-PACRG antibodies. (**C**) Chart indicating which IDAs are missing in *ida* mutants and for which mutants sliding velocities increase upon addition of anti-PACRG antibodies. (**D**) Cartoon illustrating the location of IDA subforms within the 96 nm axoneme repeat [Adapted from (Bui *et al.*, 2012)].

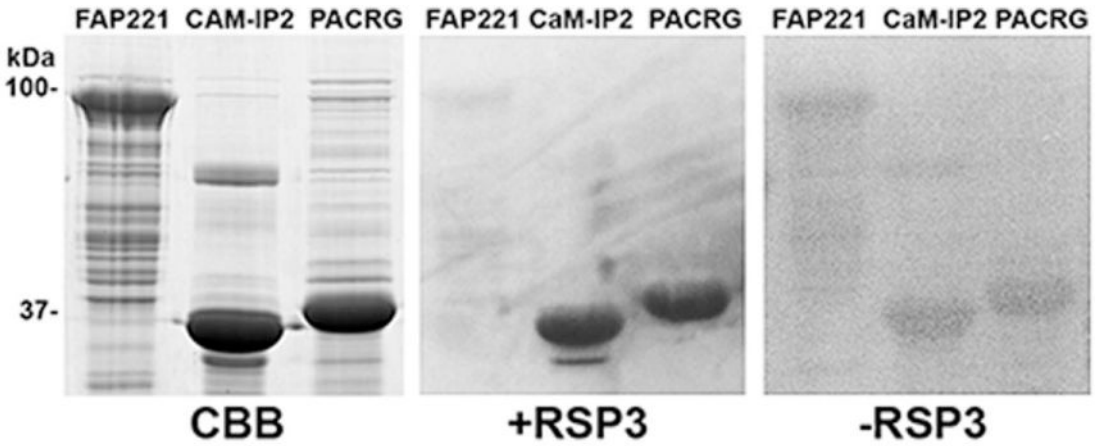

Fig. 3. Gel overlay with expressed RSP3-GST

Expressed and purified His-FAP221, His-CaM-IP2 and His-PACRG proteins were resolved on polyacrylamide gels, Coomassie blue stained (CBB) or transferred to nitrocellulose and overlaid with RSP3-GST (+RSP3) and detected using anti-GST-HRP. A blot with no RSP3-GST added was used as a GST-HRP control (−RSP3). CaM-IP2 was previously shown to interact with RSP3 (Dymek and Smith, 2007). FAP221 is a central pair component not expected to bind RSP3. RSP3-GST is able to bind full length expressed PACRG, as well as CaM-IP2.

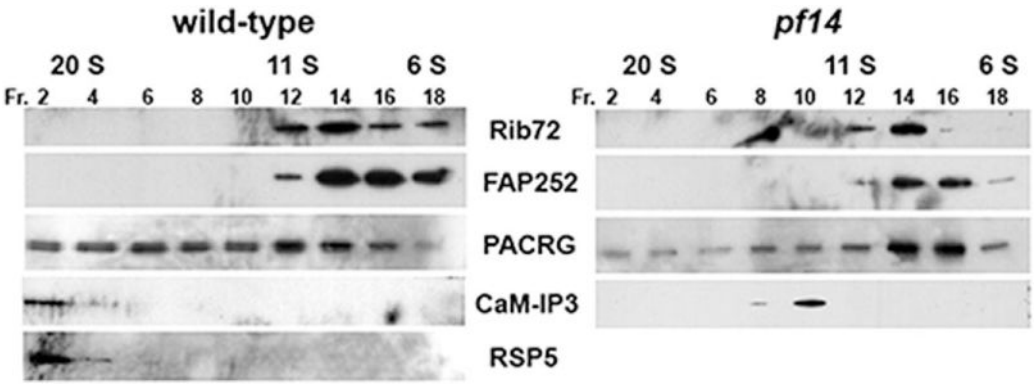

Fig. 4. Western blots of axonemal extracts fractionated on sucrose gradients

KI extracts from wild-type (left) or *pf14* (right) axonemes were fractionated on a 5–20% sucrose gradient. Fractions were collected and resolved by SDS-PAGE, transferred to a membrane and blotted with anti-Rib72, -PACRG, -FAP252, CaM-IP3, or -RSP5 antibodies. CaM-IP3, a CSC component, interacts with the RSs and sediments at 21S. In the absence of RSs, the CSC sediments at ~11S. RSP5 is a RS stalk component and does not assemble in *pf14* axonemes. PACRG sediments in a range of fractions included fractions containing RSs. In extracts lacking RSs, PACRG no longer sediments at 21S and is enriched in 6S fractions. Rib72 and FAP252 sediment between 6S and 11S using either WTor pf14 axonemal extracts.

Table I

Strain, + Antibody Addition, Sliding Velocity

Strain/antibody	μm/sec ± SEM	*n*	*P* value
wild-type	17.55 ± 1.4	50	
pf18	10.19 ± 0.3	265	
pf18 + PACRG	14.53 ± 0.6	151	<0.0001
pf18 + FAP252	14.97 ± 0.6	156	<0.0001
pf18 + Rib72	16.87 ± 0.7	159	<0.0001
pf18ida1	12.19 ± 0.4	199	
pf18ida1 + PACRG	14.30 ± 0.6	90	0.004
pf18ida1 + FAP252	17.88 ± 0.8	101	<0.0001
pf18ida1 + Rib72	18.02 ± 0.9	73	<0.0001
pf18ida4	7.77 ± 0.4	139	
pf18ida4 + PACRG	9.19 ± 0.7	50	0.09
pf18ida4 + FAP252	6.70 ± 0.5	94	0.046
pf18ida4 + Rib72	6.76 ± 0.7	53	0.20
pf18ida6	13.30 ± 0.5	100	
pf18ida6 + PACRG	14.79 ± 0.7	78	0.08
pf18ida9	12.34 ± 0.5	75	
pf18ida9 + PACRG	16.76 ± 0.7	71	<0.0001
pf18pf28	1.20 ± 0.2	15	
pf18pf28 + PACRG	0.80 ± 0.1	15	0.55
pf14	10.01 ± 0.4	194	
pf14 + PACRG	12.58 ± 0.6	86	0.0004
pf14 + FAP252	10.74 ± 0.5	134	0.23
pf14 + Rib72	12.57 ± 0.6	122	0.0007
pf14pf30	7.90 ± 0.3	161	
pf14pf30 + PACRG	12.17 ± 0.6	78	<0.0001

Table includes Chlamydomonas strains from which axonemes were isolated for the sliding assay, where and which antibody was added, and microtubule sliding velocity (μm/sec ±SEM). *P* values refer to differences between axonemes isolated from a particular strain and those axonemes with addition of a specific antibody.